Supporting Information

Versatile Electrochemical Activation Strategy for High-Performance Supercapacitor in the Model of MnO_2

Yaxiong Zhang[#], Yupeng Liu[#], Zhenheng Sun, Jiecai Fu*, Situo Cheng, Peng Cui, Jinyuan Zhou, Zhenxing Zhang, Xiaojun Pan, Weihua Han, Erqing Xie*

Key Laboratory for Magnetism and Magnetic Materials of the Ministry of Education, School of Physical Science and Technology, Lanzhou University, Lanzhou 730000, China

*Corresponding authors

Key Laboratory of Magnetism and Magnetic Materials of the Ministry of Education, Lanzhou University, Lanzhou 730000, P. R. China

E-mail: fujc@lzu.edu.cn (J. Fu); xieeq@lzu.edu.cn (E. Xie)

[#]These authors contributed equally to this work.

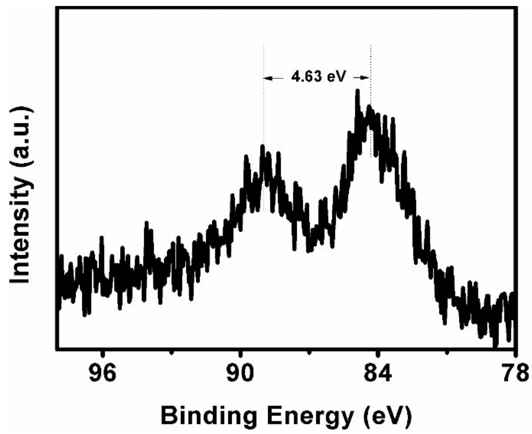

Figure S1. High resolution XPS spectra of Mn 3s for the freshly sputtered MnO_2@CNT. The peak splitting((ΔE) of Mn 3s is linearly correlated with the average oxidation state(AOS) of Mn (AOS = 8.956 − 1.126 × ΔE), and the AOS of freshly sputtered MnO_2 is about 3.7.[1, 2]

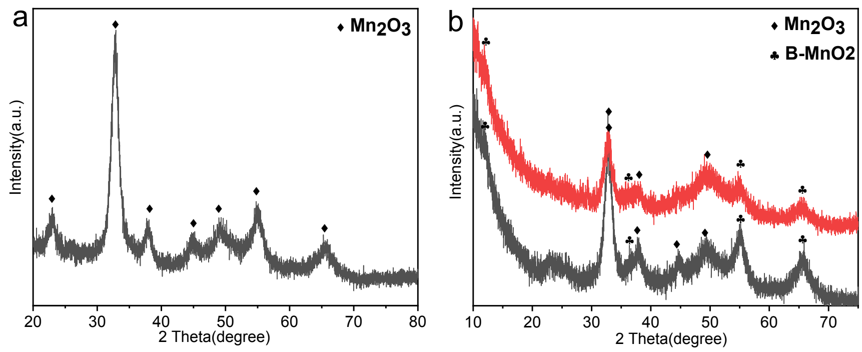

Figure S2. XRD patterns of (a) the freshly sputtered MnO_2@CNT; (b) MnO_2-NS@CNT 2C-10D after 500- (black line) and 5000-cycle (red line) electrochemical activation operations; The XRD patterns of the freshly sputtered MnO_2@CNT are readily indexed to the Mn_2O_3 (JCPDS No. 10-0069). After the electrochemical activation process, the part of XRD peaks corresponding to Mn_2O_3 disappeared, and the peaks assigned to Birnessite-MnO_2 (JCPDS No. 18-0802) appeared.

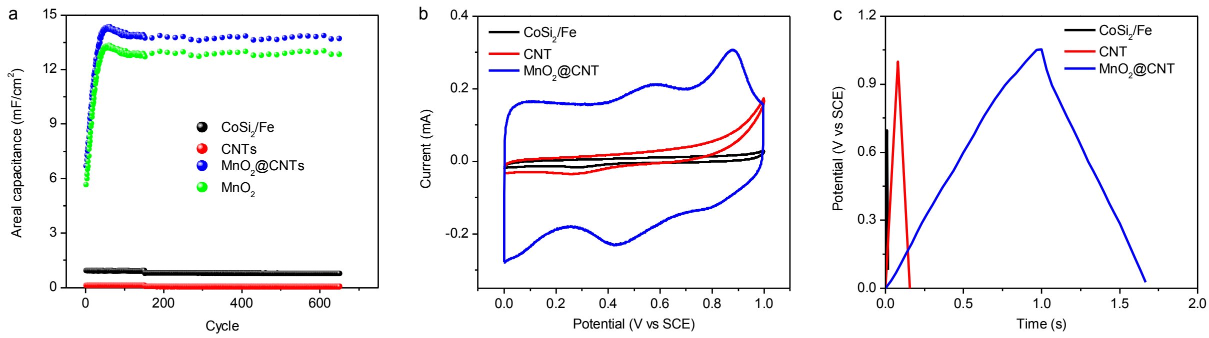

Figure S3. Electrochemical cycling performance of $CoSi_2$/Fe, CNTs, MnO_2@CNTs and MnO_2 at the current of 2 mA/cm^2.

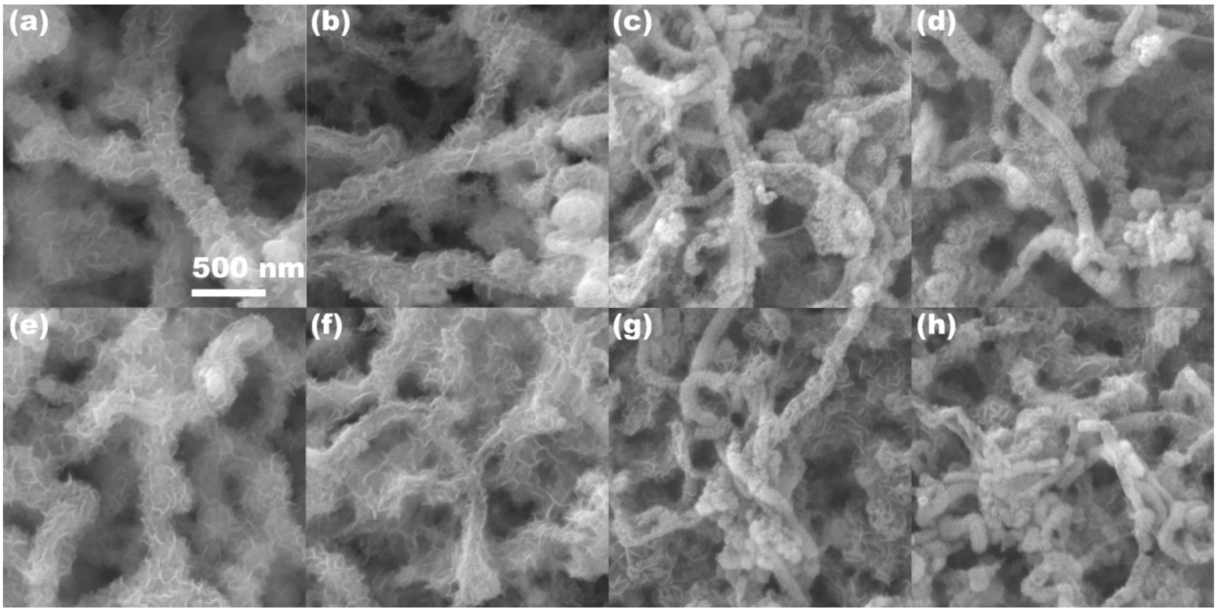

Figure S4. (a-d) SEM images of MnO_2-NS@CNTs 2C-1D, 2C-5D, 2C-10D and 2C-20D after 150 circles electrochemical activation. (e-h) SEM images of MnO_2-NS@CNTs 2C-1D, 2C-5D, 2C-10D and 2C-20D with 500 cycles electrochemical test at the current density of 10 mA/cm^2 after electrochemical activation. There is no obvious change in SEM images before and after 500 circles.

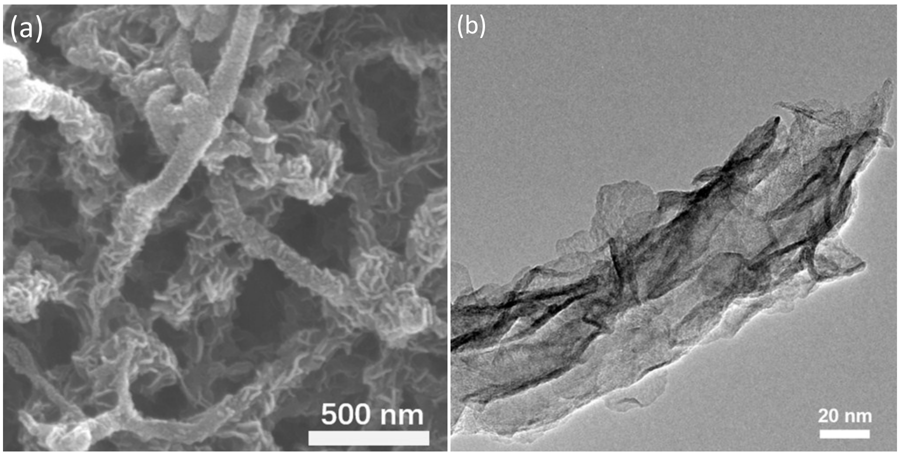

Figure S5. (a) SEM image and (b) TEM image of MnO_2-NS@CNT 2C-10D with first electrochemical activation and later 5000-cycle GCD process, respectively.

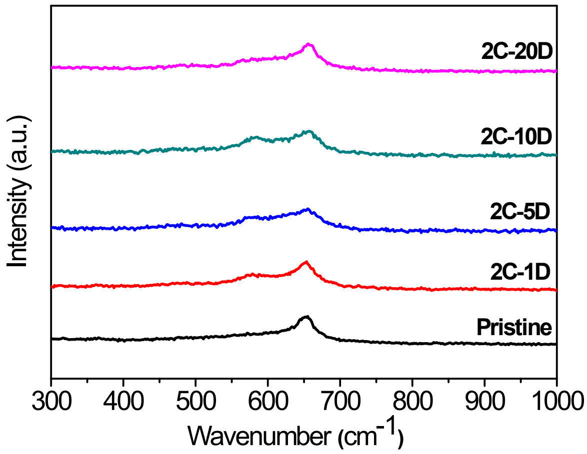

Figure S6. Raman of pristine, MnO_2-NS@CNT 2C-1D, 2C-5D, 2C-10D and 2C-20D.

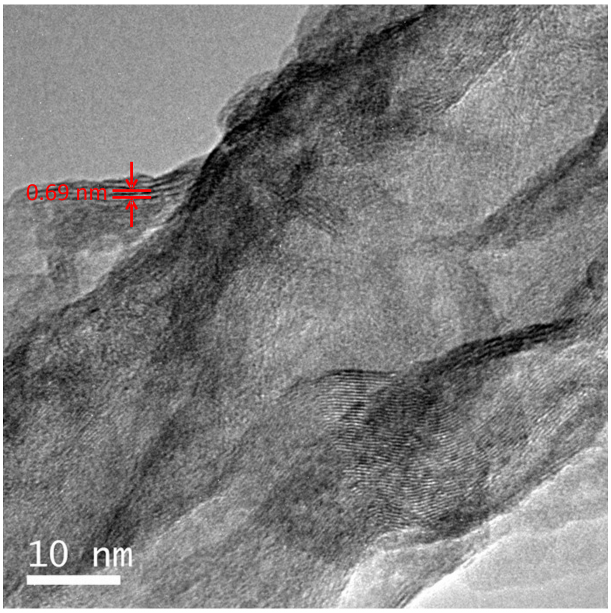

Figure S7. TEM image of MnO_2-NS@CNT 2C-10D.

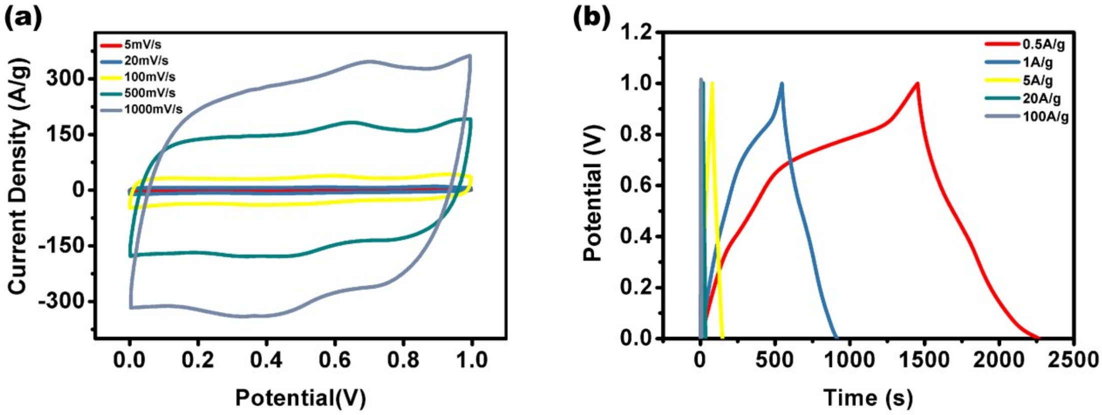

Figure S8. Electrochemical performance of MnO_2-NS@CNT 2C-10D sample. (a) CV curves at different scan rates of 5 mV/s, 20 mV/s, 100 mV/s, 500 mV/s, and 10000 mV/s. (b) GCD curves at different current density of 0.5 A/g, 1 A/g, 5 A/g, 20 A/g, and 100 A/g.

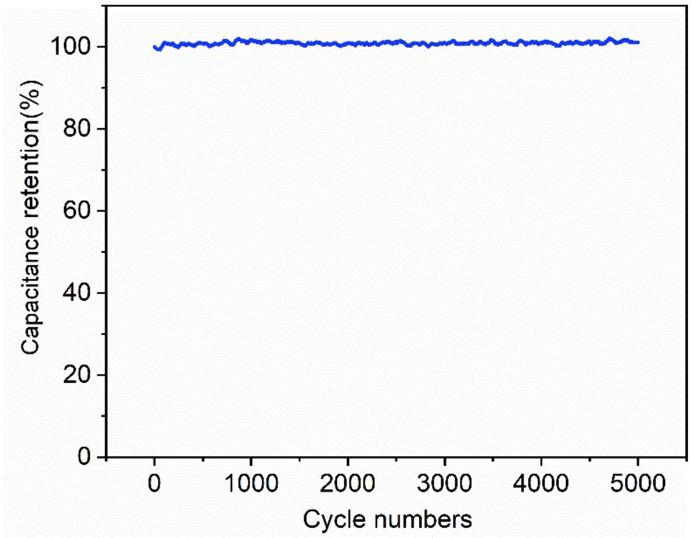

Figure S9. Electrochemical cycling performance of the electrochemically activated MnO_2-NS @CNTs 2C-10D at the current of 10 mA/cm^2.

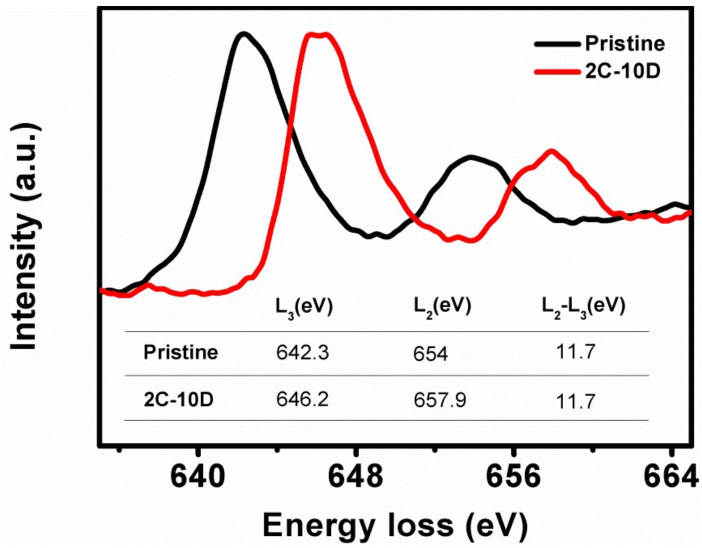

Figure S10. EELS spectra of fresh prepared MnO_2@CNTs and electrochemical activated MnO_2-NS@CNT 2C-10D.

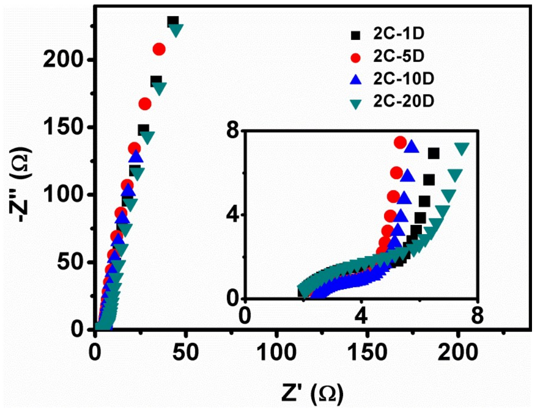

Figure S11. Nyquist plots of MnO_2-NS@CNT 2C-1D, 2C-5D, 2C-10D, and 2C-20D.

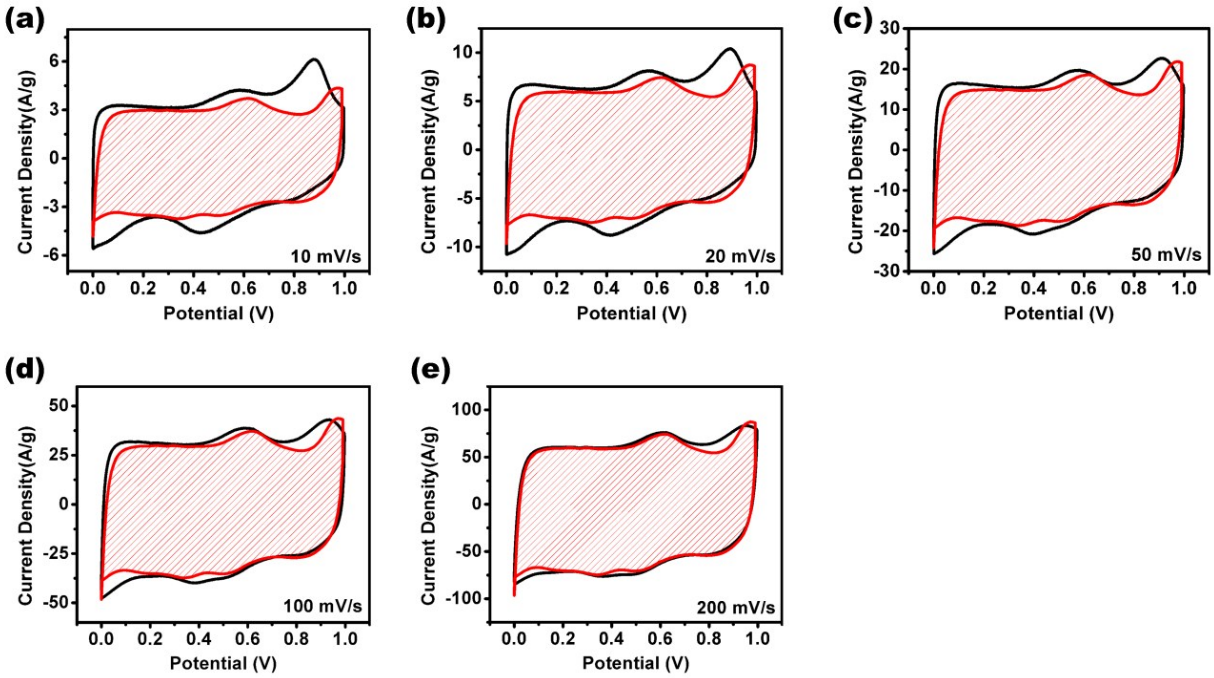

Figure S12. CV curves of the MnO_2-NS@CNT 2C-10D electrode at different scan rate, and the shadowed area represents the surface capacitive contribution**.**

Table S1. Electrochemical rate performance of Mn-based supercapacitor electrode.

Active materials	Current density change	Current density change multiple	Capacitance retention	Ref.
Co_3O_4@MnO_2	4 A/g to 20 A/g	5 times	79%	3
CNT@NCT@MnO_2	0.5 A/g to 10 A/g	20 times	45%	4
K_xMnO_2	1 A/g to 36 A/g	36 times	44%	5
Hydrophilic Carbon Cloth@MnO_2	1 A/g to 10 A/g	10 times	57%	6
MnO_2	1 A/g to 20 A/g	20 times	60%	7
Graphene/MnO_2@Conductive Wrapping	0.1 mA/cm^2 to 5 mA/cm^2	50 times	44%	8
MnO_2 film	5 mA/cm^2 to 25 mA/cm^2	5 times	15%	9
N-CNTs@MnO_2	1 A/g to 10 A/g	10 times	50%	10
$Na_{0.5}MnO_2$	1 A/g to 16 A/g	10 times	68%	11
MnO_2	1 A/g to 50 A/g	50 times	28%	12
MnO_2@CNT	0.5 A/g to 100 A/g	200 times	80%	2C-1D
MnO_2@CNT	0.5 A/g to 100 A/g	200 times	80%	2C-5D
MnO_2@CNT	0.5 A/g to 100 A/g	200 times	79%	2C-10D
MnO_2@CNT	0.5 A/g to 100 A/g	200 times	79%	2C-20D

Reference

1. X. Tan, R. Liu, C. Xie and Q. Shen, *J. Power Sources*, 2018, **374**, 134-141.
2. A. S. Poyraz, J. Huang, C. J. Pelliccione, X. Tong, S. Cheng, L. Wu, Y. Zhu, A. C. Marschilok, K. J. Takeuchi and E. S. Takeuchi, *J. Mater. Chem. A*, 2017, **5**, 16914-16928.
3. G. Liu, C. Kang, J. Fang, L. Fu, H. Zhou and Q. Liu, *J. Power Sources*, 2019, **431**, 48-54.

4. Y. Wang, D. Zhang, Y. Lu, W. Wang, T. Peng, Y. Zhang, Y. Guo, Y. Wang, K. Huo, J.-K. Kim and Y. Luo, *Carbon*, 2019, **143**, 335-342.
5. N. Jabeen, Q. Xia, S. V. Savilov, S. M. Aldoshin, Y. Yu and H. Xia, *ACS Appl. Mater. Interfaces*, 2016, **8**, 33732-33740.
6. Z. Chen, L. Zheng, T. Zhu, Z. Ma, Y. Yang, C. Wei, L. Liu and X. Gong, *Adv. Electron. Mater.*, 2019, **5**, 1800721.
7. C. Liu, Y. Chen, Z. Dong, X. Wu, Y. Situ and H. Huang, *Electrochim. Acta*, 2019, **298**, 678-684.
8. G. Yu, L. Hu, N. Liu, H. Wang, M. Vosgueritchian, Y. Yang, Y. Cui and Z. Bao, *Nano Lett.*, 2011, **11**, 4438-4442.
9. Y. Hou, Y. Cheng, T. Hobson and J. Liu, *Nano Lett.*, 2010, **10**, 2727-2733.
10. X. Ou, Q. Li, D. Xu, J. Guo and F. Yan, *Chem. Asian J.*, 2018, **13**, 545-551.
11. N. Jabeen, A. Hussain, Q. Xia, S. Sun, J. Zhu and H. Xia, *Adv. Mater.*, 2017, **29**, 1700804.
12. T. Xiong, W. S. V. Lee and J. Xue, *ACS Appl. Energy Mater.*, 2018, **1**, 5619-5626.